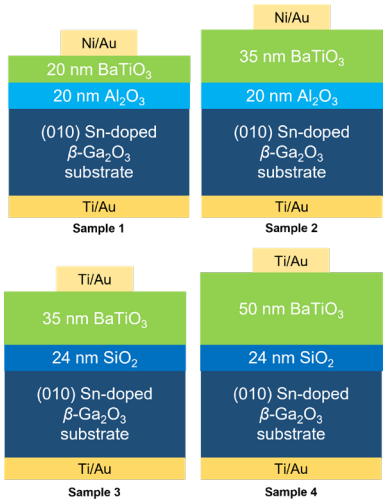

Fig. 1: Schematics of MOSCAPs studied in this work

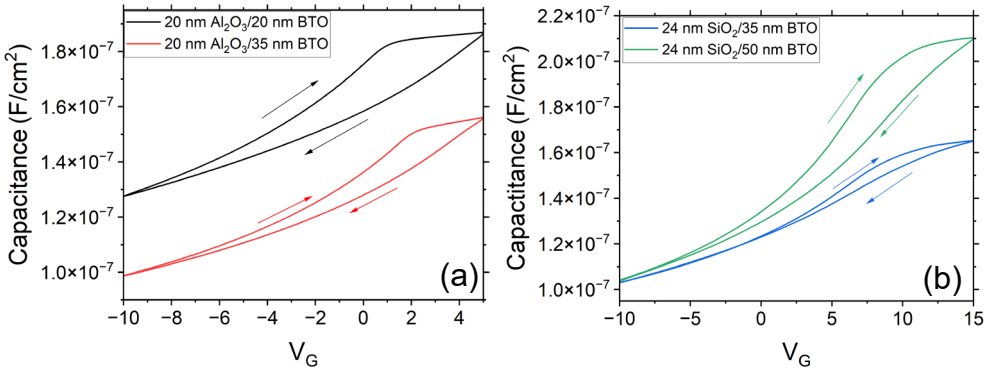

Fig. 2: Dual-sweep C-V characteristics at 1 MHz of (a) MOSCAPs with Al_2O_3 low-k layers and (b) MOSCAPs with SiO_2 low-k layer

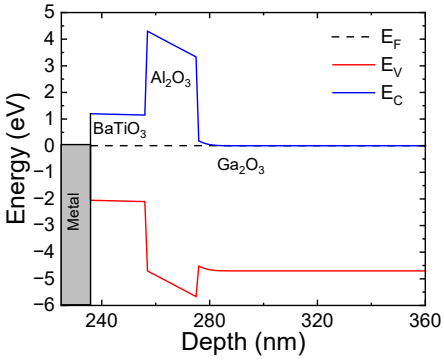

Fig. 3: Equilibrium energy band diagram of the sample with 20 nm $BaTiO_3$ and 20 nm Al_2O_3

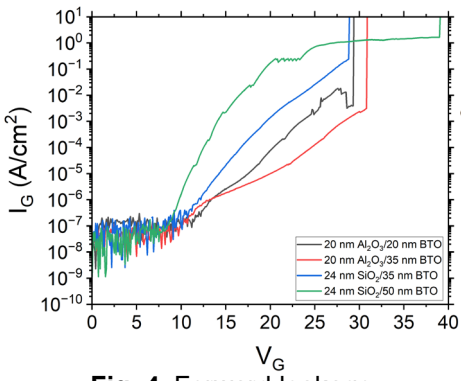

Fig. 4: Forward leakage characteristics of the four MOSCAPs

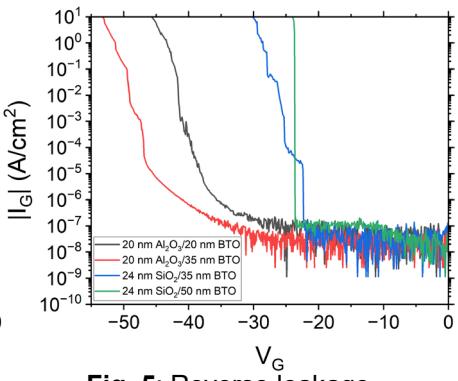

Fig. 5: Reverse leakage characteristics of the four MOSCAPs

Hybrid insulator Stack	Flat-band voltage	Net donor density from C-V	Insulator breakdown field under forward bias	Semiconductor breakdown field under reverse bias
20 nm Al_2O_3/20 nm $BaTiO_3$	0.8 V	4.4x10^{18} cm^{-3}	5.7 MV/cm	6.8 MV/cm
20 nm Al_2O_3/35 nm $BaTiO_3$	2 V	2.4x10^{18} cm^{-3}	4.7 MV/cm	5.9 MV/cm
24 nm SiO_2/35 nm $BaTiO_3$	7.9 V	5.5x10^{18} cm^{-3}	2.0 MV/cm	3.6 MV/cm
24 nm SiO_2/50 nm $BaTiO_3$	7.8 V	5.3x10^{18} cm^{-3}	0.9 MV/cm	3.5 MV/cm

Table 1: Summary of flat-band voltage, extracted doping density, forward breakdown field in oxide, and reverse breakdown field supported in Ga_2O_3 for all four samples